The Astrophysical Journal, 719:612–621, 2010 August 10 doi:10.1088/0004-637X/719/1/612

EVOLUTION OF WHITE DWARF STARS WITH HIGH-METALLICITY PROGENITORS: THE ROLE OF ^{22}Ne DIFFUSION

L. G. Althaus[1,2,3], E. García-Berro[2,4], I. Renedo[2,4], J. Isern[4,5], A. H. Córsico[1,3], and R. D. Rohrmann[6]
[1] Facultad de Ciencias Astronómicas y Geofísicas, Universidad Nacional de La Plata, Paseo del Bosque s/n, 1900 La Plata, Argentina; althaus@fcaglp.unlp.edu.ar
[2] Departament de Física Aplicada, Universitat Politècnica de Catalunya, c/Esteve Terrades 5, 08860 Castelldefels, Spain
[3] Instituto de Astrofísica de La Plata, IALP (CCT La Plata), CONICET-UNLP, Argentina
[4] Institut d'Estudis Espacials de Catalunya, c/Gran Capità, 2-4, Edif. Nexus 104, 08034 Barcelona, Spain
[5] Institut de Ciències de l'Espai (CSIC), Campus UAB, Facultat de Ciències, Torre C-5, 08193 Bellaterra, Spain
[6] Instituto de Ciencias Astronómicas, de la Tierra y del Espacio, CONICET, Av. de España 1512 (Sur), CC 49 (5500) San Juan, Argentina
Received 2010 May 7; accepted 2010 June 21; published 2010 July 21

ABSTRACT

Motivated by the strong discrepancy between the main-sequence turnoff age and the white dwarf cooling age in the metal-rich open cluster NGC 6791, we compute a grid of white dwarf evolutionary sequences that incorporates for the first time the energy released by the processes of ^{22}Ne sedimentation and of carbon/oxygen phase separation upon crystallization. The grid covers the mass range from 0.52 to 1.0 $M_{\odot}$, and is appropriate for the study of white dwarfs in metal-rich clusters. The evolutionary calculations are based on a detailed and self-consistent treatment of the energy released from these two processes, as well as on the employment of realistic carbon/oxygen profiles, of relevance for an accurate evaluation of the energy released by carbon/oxygen phase separation. We find that ^{22}Ne sedimentation strongly delays the cooling rate of white dwarfs stemming from progenitors with high metallicities at moderate luminosities, while carbon/oxygen phase separation adds considerable delays at low luminosities. Cooling times are sensitive to possible uncertainties in the actual value of the diffusion coefficient of ^{22}Ne. Changing the diffusion coefficient by a factor of 2 leads to maximum age differences of ≈8%–20% depending on the stellar mass. We find that the magnitude of the delays resulting from chemical changes in the core is consistent with the slowdown in the white dwarf cooling rate that is required to solve the age discrepancy in NGC 6791.

Key words: dense matter – diffusion – stars: abundances – stars: evolution – stars: interiors – white dwarfs

Online-only material: color figures

1. INTRODUCTION

The evolution of white dwarf stars is a relatively well-understood process that can be basically described as a simple cooling problem (Mestel 1952) in which the decrease in the thermal heat content of the ions constitutes the main source of luminosity. Because of this, white dwarfs can be used as independent reliable cosmic clocks to date a wide variety of stellar populations. This fact has attracted the attention of numerous researchers over the years, who have devoted large efforts to study in detail the evolutionary properties of these stars. In particular, it is important to realize that an accurate determination of the rate at which white dwarfs cool down constitutes a fundamental issue. Detailed evolutionary models for these stars, based on increasing degrees of sophistication of their constitutive physics and energy sources, have proved to be valuable at determining interesting properties of many Galactic populations, including the disk (Winget et al. 1987; García-Berro et al. 1988a; Hernanz et al. 1994; García-Berro et al. 1999), the halo (Isern et al. 1998; Torres et al. 2002), and globular and open clusters (Richer et al. 1997; Von Hippel & Gilmore 2000; Hansen et al. 2002, 2007; Von Hippel et al. 2006; Winget et al. 2009). This important application of white dwarf stars has also been possible thanks to a parallel effort devoted to the empirical determination of the observed white dwarf cooling sequences in stellar clusters, as well as the determination of the luminosity function of field white dwarfs, which also provides a measure of the white dwarf cooling rate.

Detailed models of white dwarfs require a complete treatment of the energy sources resulting from the core crystallization. In particular, the release of both latent heat (Van Horn 1968; Lamb & Van Horn 1975) and gravitational energy due to the change in chemical composition induced by crystallization (Stevenson 1980; García-Berro et al. 1988b; Segretain et al. 1994; Isern et al. 1997, 2000) considerably affects the cooling of white dwarfs. In particular, compositional separation at crystallization markedly slows down the cooling. This in turn influences, for instance, the position of the cutoff of the disk white dwarf luminosity function (Hernanz et al. 1994), which is essential in obtaining an independent determination of the age of the Galactic disk.

However, a new observational determination of the white dwarf luminosity function of the cluster NGC 6791 by Bedin et al. (2008) casts serious doubts on the reliability of existing white dwarf evolutionary models and their use as accurate clocks. NGC 6791 is a very old (8 Gyr) and very metal-rich ([Fe/H] ∼ + 0.4) open cluster, for which Bedin et al. (2008) have uncovered the faint end of the white dwarf cooling track, and have convincingly demonstrated the existence of a peak and a subsequent cutoff in the white dwarf luminosity function at $m_{\rm F606W} \approx 28.15$. Additionally, Bedin et al. (2008) have found that the age of the cluster derived from the main-sequence turnoff technique (8 Gyr) is in serious conflict with the age derived from the termination of the cooling sequence (6 Gyr). This discrepancy has strong implications for the theory of white dwarf evolution, and points out at a missing piece of physics in the conventional modeling of white dwarfs. In particular, Bedin et al. (2008) have concluded that the white dwarfs in NGC 6791 have to cool markedly more slowly than believed in order to reproduce the faint peak and measured cutoff in the observed white dwarf luminosity function at the age of the cluster derived from the well-established main-sequence turnoff technique.

In view of the high metallicity characterizing NGC 6791 ($Z \approx 0.04$), a viable physical process that can appreciably decrease the cooling rate of white dwarfs is the slow gravitational settling of ^{22}Ne in the liquid phase. ^{22}Ne is the most abundant impurity expected in the carbon–oxygen interiors of typical white dwarfs. Its abundance by mass reaches $X_{\rm Ne} \approx Z_{\rm CNO}$, and it is the result of helium burning on ^{14}N—built up during the CNO cycle of hydrogen burning. As first noted by Bravo et al. (1992), the two extra neutrons present in the ^{22}Ne nucleus (relative to $A_i = 2Z_i$ nuclei, where A_i is the atomic mass number and Z_i is the charge) result in a net downward gravitational force of magnitude $2m_p g$, where g is the local gravitational acceleration and m_p is the proton mass. This leads to a slow, diffusive settling of ^{22}Ne in the liquid regions toward the center of the white dwarf. The role of ^{22}Ne sedimentation in the energetics of crystallizing white dwarfs was first addressed by Isern et al. (1991) and more recently quantitatively explored by Deloye & Bildsten (2002) and García-Berro et al. (2008), who concluded that ^{22}Ne sedimentation releases sufficient energy to affect appreciably the cooling of massive white dwarfs, making them appear bright for very long periods of time, of the order of 10^9 yr. Deloye & Bildsten (2002) predicted that the possible impact of ^{22}Ne sedimentation on white dwarf cooling could be better seen in metal-rich clusters, such as NGC 6791, where the neon abundance expected in the cores of white dwarfs could be as high as ∼4% by mass.

The effect of ^{22}Ne sedimentation is not included in any of the existing grids of white dwarf evolutionary calculations, and its effect on the evolution of white dwarfs resulting from supersolar metallicity progenitors has not been addressed. The only study of the effects of ^{22}Ne sedimentation in the cooling of white dwarfs using a complete stellar evolutionary code is that of García-Berro et al. (2008) for the case of solar metallicity. In this paper, we present the first grid of full white dwarf evolutionary models resulting from metal-rich progenitors with masses ranging from 1 to 5 $M_\odot$ that includes both ^{22}Ne sedimentation and carbon–oxygen phase separation. This grid incorporates a much more elaborated and improved treatment of the physical processes relevant for the white dwarf evolution than that which we considered in García-Berro et al. (2008). These improvements include, in addition to an update in the microphysics content, the derivation of starting white dwarf configurations obtained from a full calculation of the progenitor evolution, as well as a precise and self-consistent treatment of the energy released by the redistribution of carbon and oxygen due to phase separation during crystallization, which was lacking in our previous study. We find that the energy released by ^{22}Ne sedimentation markedly impacts the evolution of white dwarfs populating metal-rich clusters, and that this source of energy must be taken into account in deriving stellar ages from the white dwarf cooling sequence of such clusters. In particular, at the evolutionary stages where the faint peak and cutoff of the white dwarf luminosity function of NGC 6791 are observed, we find that the release of energy from both phase separation and ^{22}Ne sedimentation substantially slows down the cooling of white dwarfs. The occurrence of these physical separation processes in the core of cool white dwarfs and the associated slowdown of the cooling rate have recently been demonstrated by García-Berro et al. (2010) to be a fundamental aspect to reconcile the age discrepancy in NGC 6791.

In this study, there are three distinctive characteristics that allow us to obtain absolute ages for white dwarfs in metal-rich clusters. First, as already mentioned, the inclusion of the energy released from both ^{22}Ne sedimentation and carbon–oxygen phase separation is done self-consistently and locally coupled to the full set of equations of stellar evolution. In addition, realistic carbon–oxygen profiles expected in the cores of white dwarfs, of relevance for an accurate evaluation of the energy released by phase separation, are derived from the full computation of the evolution of progenitor stars. Finally, detailed non-gray model atmospheres are used to derive the outer boundary conditions of our evolving sequences. All these facts allow us to obtain accurate ages. The paper is organized as follows. In Section 2 we give a full account of the input physics of our evolutionary code, particularly the treatment of the energy sources. In Section 3 we present our results, and finally in Section 4 we summarize our findings and draw our conclusions.

2. DETAILS OF COMPUTATIONS

2.1. Input Physics

Evolutionary calculations for both the white dwarfs and the progenitor stars were done with an updated version of the LPCODE stellar evolutionary code—see Althaus et al. (2005a) and references therein. This code has recently been employed to study different aspects of the evolution of low-mass stars, such as the formation and evolution of H-deficient white dwarfs, PG 1159, and extreme horizontal branch stars (Althaus et al. 2005a, 2009a; Miller Bertolami & Althaus 2006; Miller Bertolami et al. 2008), as well as the evolution of He-core white dwarfs with high-metallicity progenitors (Althaus et al. 2009b). It has also been used to study the initial–final mass relation in Salaris et al. (2009), where a test and comparison of LPCODE with other evolutionary codes has also been made. Details of LPCODE can be found in these works. In what follows, we comment on the main input physics that are relevant for the evolutionary calculations presented in this work.

The LPCODE evolutionary code considers a simultaneous treatment of non-instantaneous mixing (or extra-mixing if present) and burning of elements (Althaus et al. 2003). The nuclear network accounts explicitly for 16 chemical elements, and the thermonuclear reaction rates are those described in Althaus et al. (2005a), with the exception of $^{12}{\rm C} + p \rightarrow {}^{13}{\rm N} + \gamma \rightarrow {}^{13}{\rm C} + e^+ + \nu_{\rm e}$ and $^{13}{\rm C}(p,\gamma)^{14}{\rm N}$, which are taken from Angulo et al. (1999). The $^{12}{\rm C}(\alpha,\gamma)^{16}{\rm O}$ reaction rate is taken from Angulo et al. (1999) as well, and is about twice as large as that of Caughlan & Fowler (1988). The final carbon–oxygen composition is a relevant issue, as a proper computation of the energy released by phase separation markedly depends on the chemical profile of the core. The standard mixing length theory for convection—with the free parameter $\alpha = 1.61$—has been adopted. With this value, the present luminosity and effective temperature of the Sun, at an age of 4570 Myr, are reproduced by LPCODE when $Z = 0.0164$ and $X = 0.714$ are adopted—in agreement with the Z/X value of Grevesse & Sauval (1998).

Except for the evolutionary stages corresponding to the thermally pulsing (TP) asymptotic giant branch (AGB) phase, we considered the occurrence of extra-mixing episodes beyond each convective boundary following the prescription of Herwig et al. (1997). Extra-mixing episodes largely determine the final chemical profile of white dwarfs. We treated extra-mixing as a diffusion process by assuming that mixing velocities decay exponentially beyond each convective boundary. Specifically, we assumed a diffusion coefficient given by $D_{\rm OV} = D_{\rm O} \exp(-2z/f H_{\rm P})$, where $H_{\rm P}$ is the pressure scale height at the convective boundary, $D_{\rm O}$ is the diffusion

coefficient of unstable regions close to the convective boundary, and z is the geometric distance from the edge of the convective boundary (Herwig et al. 1997). We adopted $f = 0.016$ in all of our sequences, a value inferred from the width of the upper main sequence.

Other physical ingredients considered in LPCODE are the radiative opacities from the OPAL project (Iglesias & Rogers 1996), including C- and O-rich composition, supplemented at low temperatures with the molecular opacities of Alexander & Ferguson (1994). During the white dwarf regime, the metal mass fraction Z in the envelope is not assumed to be fixed. Instead, it is specified consistently according to the prediction of element diffusion. To account for this, we have considered radiative opacity tables from OPAL for arbitrary metallicities. For effective temperatures less than 10,000 K, we have included the effects of molecular opacity by assuming pure hydrogen composition from the computations of Marigo & Aringer (2009). This assumption is justified because element diffusion leads to pure hydrogen envelopes in cool white dwarfs. It is worth noting that these opacity calculations do not cover the high-density regime characteristic of the envelopes of cool white dwarfs. Nevertheless, because the derivation of the outer boundary conditions for our evolving models involves the integration of detailed non-gray model atmospheres down to very large optical depths ($\tau = 25$), these opacities are only required at large τ and low effective temperatures. However, at the high densities reached at the end of the atmospheric integration, energy transfer is mainly by convection, which at such depths is essentially adiabatic. Indeed, we find that at $\tau = 25$, the radiative flux amounts to 4% at most. Consequently, the temperature stratification characterizing these deep layers becomes strongly tied to the equation of state, so a detailed knowledge of the radiative opacity becomes almost irrelevant. The conductive opacities are those of Cassisi et al. (2007), and the neutrino emission rates are taken from Itoh et al. (1996) and Haft et al. (1994). For the high-density regime characteristics of white dwarfs, we have used the equation of state of Segretain et al. (1994), which accounts for all the important contributions for both the liquid and solid phases—see Althaus et al. (2007) and references therein. We have also considered the abundance changes resulting from element diffusion in the outer layers of white dwarfs. As a result, our sequences develop pure hydrogen envelopes, the thickness of which gradually increases as evolution proceeds. We have considered gravitational settling and thermal and chemical diffusion; see Althaus et al. (2003) for details. In LPCODE, diffusion becomes operative once the wind limit is reached at high effective temperatures (Unglaub & Bues 2000). Chemical rehomogenization of the inner carbon–oxygen profile induced by Rayleigh–Taylor instabilities has been considered following Salaris et al. (1997). These instabilities arise because the positive molecular weight gradients that remain above the flat chemical profile left by convection during core helium burning.

Finally, we employ outer boundary conditions for our evolving white dwarf models as provided by detailed non-gray model atmospheres that include non-ideal effects in the gas equation of state and chemical equilibrium based on the occupation probability formalism. The level occupation probabilities are self-consistently incorporated in the calculation of the line and continuum opacities. Model atmospheres also consider collision-induced absorption due to H_2–H_2, H_2–He, and H–He pairs, and the Lyα quasi-molecular opacity that results from perturbations of hydrogen atoms by interactions with other particles, mainly H and H_2. These model atmospheres have been developed by Rohrmann et al. (2002, 2010), and we refer the reader to those works and to Renedo et al. (2010) for a full description of them. In the interest of reducing computing time, we have computed from these models a grid of pressure, temperature, radial thickness, and outer mass fraction values at an optical depth $\tau = 25$ from which we derive the outer boundary conditions. At advanced stages of white dwarf evolution, the central temperature becomes strongly tied to the temperature stratification of the very outer layers, thus the employment of non-gray model atmospheres is highly desired for an accurate assessment of cooling times of cool white dwarfs (Prada Moroni & Straniero 2007). Our model atmospheres also provide detailed colors and magnitudes for effective temperatures lower than 60,000 K for a pure hydrogen composition and for the *Hubble Space Telescope* Advanced Camera for Surveys filters (Vega-mag system) and *UBVRI* photometry.

2.1.1. Energy Released from ^{22}Ne Sedimentation and Crystallization

The energy contribution resulting from the gravitational settling of ^{22}Ne is treated in a similar way as was done in García-Berro et al. (2008), except that now we have assumed that the liquid behaves as a single-background, one-component plasma consisting of the average by number of carbon and oxygen—the inner chemical composition expected in a real white dwarf—plus traces of ^{22}Ne. This allows us to treat the problem of ^{22}Ne diffusion in a simple and realistic way. The slow change in the ^{22}Ne chemical profile and the associated local contribution to the luminosity equation is provided by an accurate treatment of time-dependent ^{22}Ne diffusion; see García-Berro et al. (2008) for details. In particular, the diffusion coefficient D_s in the liquid interior is given by (Deloye & Bildsten 2002)

$$D_s = 7.3 \times 10^{-7} \frac{T}{\rho^{1/2} \overline{Z}\, \Gamma^{1/3}} \ \mathrm{cm^2\, s^{-1}}, \qquad (1)$$

where we have considered a mean charge $\overline{Z}$ of the background plasma. For those regions of the white dwarf that have been crystallized, diffusion is expected to be no longer efficient due to the abrupt increase in viscosity expected in the solid phase. Thus, we set $D = 0$ in the crystallized regions.

In a subsequent phase, we have also considered the energy sources resulting from the crystallization of the white dwarf core, i.e., the release of latent heat and the release of gravitational energy associated with carbon–oxygen phase separation induced by crystallization. In LPCODE, these energy sources are included self-consistently and are locally coupled to the full set of equations of stellar evolution. In particular, the standard luminosity equation

$$\frac{\partial L_r}{\partial M_r} = \varepsilon_{\mathrm{nuc}} - \epsilon_\nu - C_P \frac{dT}{dt} + \frac{\delta}{\rho} \frac{dP}{dt} \qquad (2)$$

had to be modified. In Equation (2), $\varepsilon_{\mathrm{nuc}}$ and ϵ_ν denote, respectively, the energy per unit mass per second due to nuclear burning and neutrino losses, and the third and fourth terms are the well-known contributions of the heat capacity and pressure changes to the local luminosity of the star (Kippenhahn & Weigert 1990). We have simplified the treatment of phase separation by ignoring the presence of ^{22}Ne. As shown by Segretain (1996), ^{22}Ne influences the phase diagram at the late stages of crystallization, and the impact on the cooling time is moderate and much smaller than that resulting from

carbon–oxygen phase separation. Thus, to compute the energy resulting from phase separation, we assume that the white dwarf interior is made only of carbon and oxygen with abundance by mass X_C and X_O, respectively ($X_C + X_O = 1$). Then, it can be shown (García-Berro et al. 2008) that

$$\frac{\partial L_r}{\partial M_r} = \varepsilon_{\rm nuc} - \epsilon_\nu - C_P\frac{dT}{dt} + \frac{\delta}{\rho}\frac{dP}{dt} + l_s\frac{dM_s}{dt}\delta(m - M_s) - A\frac{dX_O}{dt}, \quad (3)$$

where A is given by

$$A = \left(\frac{\partial u}{\partial X_O}\right)_{\rho,T} + \frac{\delta}{\rho}\left(\frac{\partial P}{\partial X_O}\right)_{\rho,T} \approx \left(\frac{\partial u}{\partial X_O}\right)_{\rho,T}, \quad (4)$$

u being the internal energy per gram.

The fifth term in Equation (3) is the local contribution of latent heat: l_s is the latent heat of crystallization and dM_s/dt is the rate at which the solid core grows. The delta function indicates that the latent heat is released at the solidification front. The last term in Equation (3) represents the energy released by chemical abundance changes. Although this term is usually small in normal stars, since it is much smaller than the energy released by nuclear reactions, it plays a major role in crystallizing white dwarfs, with important energetic consequences due to carbon–oxygen phase separation. In the case of carbon–oxygen mixtures, $(\partial u/\partial X_O)_{\rho,T}$ is dominated by the ionic contributions, and is negative. Hence, the last term in Equation (3) will be a source (sink) of energy in those regions where the oxygen abundance increases (decreases). During the crystallization of a carbon–oxygen white dwarf, the oxygen abundance in the crystallizing region increases, and the overlying liquid mantle becomes carbon-enriched as a result of a mixing process induced by a Rayleigh–Taylor instability at the region above the crystallized core. Thus, according to Equation (3), phase separation will lead to a source of energy in those layers that are crystallizing, and to a sink of energy in the overlying layers. We computed the resulting chemical rehomogenization following the prescription by Salaris et al. (1997; see also Montgomery et al. 1999).

To implement the energy release by phase separation in our code in a suitable formalism, and to avoid numerical difficulties when integrating the full set of equations of stellar structure and evolution, we have considered the net energy released by the process of carbon–oxygen phase separation over a time interval dt, by integrating the last term in Equation (3) over the whole star. Because cooling is a slow process, it can be shown that (Isern et al. 1997)

$$\int_0^M \left(\frac{\partial u}{\partial X_O}\right)\frac{dX_O}{dt}\,dM_r = \left(X_O^{\rm sol} - X_O^{\rm liq}\right) \times \left[\left(\frac{\partial u}{\partial X_O}\right)_{M_s} - \left\langle\frac{\partial u}{\partial X_O}\right\rangle\right]\frac{dM_s}{dt}, \quad (5)$$

where $(\partial u/\partial X_O)_{M_s}$ is evaluated at the boundary of the solid core and

$$\left\langle\frac{\partial u}{\partial X_O}\right\rangle = \frac{1}{\Delta M}\int_{\Delta M}\left(\frac{\partial u}{\partial X_O}\right)dM_r. \quad (6)$$

The first term in the square bracket in Equation (5) represents the energy released in the crystallizing layer, and the second term, given by Equation (6), is the energy absorbed on average in the convective region (ΔM) driven by the Rayleigh–Taylor instability above the crystallization front. Since $(\partial u/\partial X_O)$ is negative and essentially depends on the density (which decreases outward), the square bracket is negative, and thus the process of phase separation results in a net release of energy during the time interval dt. It is clear that the energy released by this process will depend on the initial oxygen profile at the beginning of the white dwarf phase, resulting in a smaller contribution in the case of initially higher oxygen abundances. Note that the shape of the initial chemical profile may also affect the degree of mixing in the liquid layers and thus the energy absorbed there, hence altering the net energy released by the process.

For computational purposes, we proceed as follows. At each evolutionary time step, we compute the change of chemical composition resulting from carbon–oxygen phase separation using the spindle-type phase diagram for a carbon–oxygen mixture of Segretain & Chabrier (1993). Then, we evaluate the net energy released by this process during the time step from Equation (5). This energy is added to the, usually smaller, latent heat contribution, of the order of $0.77k_BT$ per ion. The resulting energy is distributed over a small mass range around the crystallization front, and the resulting local contribution is added to the luminosity equation, Equation (2). Finally, we also add to this equation the contribution from ^{22}Ne sedimentation in the same way as in García-Berro et al. (2008). The LPCODE stellar evolutionary code solves iteratively the full set of equations for the white dwarf evolution with the luminosity equation modified as previously explained. We mention that the magnitude of these energy sources is calculated at each iteration during the convergence of the model. In our calculations, crystallization sets in when the ion coupling constant reaches $\Gamma = 180$, where $\Gamma \equiv \langle Z^{5/3}\rangle e^2/a_e k_B T$ and a_e is the interelectronic distance.

Finally, we want to mention that our treatment is not entirely consistent in the sense that the energy resulting from ^{22}Ne sedimentation is evaluated separately and independently of the ^{22}Ne abundance changes induced by crystallization. However, as shown by Segretain (1996), the neon concentration is expected to change appreciably only when ~70% of the white dwarf has crystallized. Because the luminosity contribution from ^{22}Ne sedimentation strongly declines by the time a large fraction of the mass of the white dwarf has crystallized, we expect that this inconsistency in our treatment is not relevant. In any case, it should be noted that this picture could change appreciably for the case of larger initial neon abundances than that considered in Segretain (1996).

2.2. Evolutionary Sequences

As we mentioned, initial models for our white dwarf sequences have been derived from full evolutionary calculations of progenitor stars for solar metallicity (Renedo et al. 2010). All of the sequences have been computed from the zero-age main sequence (ZAMS) through the TP and mass-loss phases on the AGB and, finally, to the domain of planetary nebulae. Extra-mixing episodes beyond the pulse-driven convection zone have been disregarded during the TP-AGB phase, as suggested by different and recent studies (see Salaris et al. 2009; Weiss & Ferguson 2009 and references therein). As a result, the efficiency of the third dredge-up episode is strongly reduced for the low-mass sequences (but not for the massive ones), and thus the mass of the hydrogen-free core of our less massive sequences gradually grows as evolution proceeds through this stage. A strong reduction of extra-mixing during the AGB phase and the

resulting reduction in the efficiency of third dredge-up episodes in low-mass stars is in agreement with observational inferences of AGB carbon stars, the luminosities of which, in turn, are in good agreement with those predicted by stellar models using the Schwarzschild's criterion for convection (Guandalini et al. 2006). The breathing pulse instability occurring toward the end of core helium burning was suppressed (see Straniero et al. 2003 for a thorough discussion on this issue). We considered mass-loss episodes during the stages of core helium burning and red giant branch following Schröder & Cuntz (2005), whereas during the AGB and TP-AGB phases we used the mass-loss prescription of Vassiliadis & Wood (1993). In the case of a strong reduction of the third dredge-up efficiency, as occurs in our less massive sequences, mass loss plays a major role in determining the final mass of the hydrogen-free core at the end of the TP-AGB evolution, and thus the initial–final mass relation (Weiss & Ferguson 2009). However, we stress that the initial–final mass relation obtained from our sequences (Renedo et al. 2010) is in very good agreement with the semi-empirical determination of this relation of Salaris et al. (2009) and with that of Catalán et al. (2008). Finally, we mention that the hydrogen envelope masses of our sequences should be considered as upper limits to the maximum mass of hydrogen left in a white dwarf resulting from the evolution of single star progenitors. This stems from the fact that the occurrence of a late thermal pulse after departure from the TP-AGB may reduce the hydrogen mass considerably; see Althaus et al. (2005b). Hence, this could alter the quantitative effect of ^{22}Ne sedimentation on the white dwarf cooling.

The computation of the progenitor evolution provides realistic initial models and, more importantly, detailed carbon–oxygen chemical profiles, which are relevant for a proper computation of the energy released by carbon–oxygen phase separation. In Figure 1, we show the mass abundances of ^{1}H, ^{4}He, ^{12}C, and ^{16}O throughout the deep interior of a selected 0.7051 $M_{\odot}$ white dwarf model at an evolutionary stage where element diffusion has already strongly modified the initial outer layer chemical stratification, leading to the formation of a thick pure hydrogen envelope plus an extended inner tail. Below the hydrogen envelope there is the helium buffer and an intershell rich in helium, carbon, and oxygen. Finally, the innermost region is mainly composed of carbon and oxygen, plus traces of heavier elements of which ^{22}Ne is the most abundant one. As previously mentioned, ^{22}Ne is the result of helium burning on ^{14}N via the reactions ^{14}N$(\alpha,\gamma)^{18}$F$(\beta^{+})^{18}$O$(\alpha,\gamma)^{22}$Ne. The core chemical profile of our model is typical of situations in which extra mixing episodes beyond the fully convective core during the core He burning are allowed, see Straniero et al. (2003) and also Prada Moroni & Straniero (2007) for the consequences on white dwarf evolution. The flat chemical profile toward the center is the result of the chemical rehomogenization induced by Rayleigh–Taylor instabilities.

In this work, we have considered two initial ^{22}Ne abundances of $X_{\rm Ne} \approx Z_{\rm CNO} \approx 0.03$ and 0.06. These values are not entirely consistent with the almost solar metallicity we assumed for the progenitor stars, $Z = 0.01$. This introduces a slight inconsistency, however, since only a minor difference is expected in the oxygen composition and in the white dwarf evolution when progenitors with different metallicities are considered (Prada Moroni & Straniero 2002; Salaris et al. 2010). Thus, to a good approximation, our starting models are representative of white dwarf stars with progenitors having supersolar metallicity. However, we mention that a significant change in the metallicity progenitor could affect the AGB evolution and mass-loss history, as well as the initial–final mass relation. In this work, we computed white dwarf sequences with hydrogen-rich envelopes for ^{22}Ne abundances of 0.03 and 0.06, taking into account the energy contributions from ^{22}Ne sedimentation and carbon–oxygen phase separation. We also compute additional sequences to assess the impact of these energy sources. This includes the computation of the evolution of a 1.0 $M_{\odot}$ white dwarf sequence that was started, in contrast to the other sequences, from an artificially generated initial model, and with a carbon–oxygen composition similar to that of the 0.8779 $M_{\odot}$ sequence. In this way, our sequences cover the entire white dwarf mass interval for which a carbon–oxygen core is expected to be formed. In Table 1, we list the stellar masses of the white dwarfs for which we compute their progenitor evolution, together with the initial masses of the progenitor stars at the ZAMS. Also listed in Table 1 is the central oxygen abundance at the beginning of the white dwarf evolutionary track. These sequences were computed from the pre-white-dwarf stage down to $\log(L/L_{\odot}) \approx -5.3$. To explore the relevance for the cooling times of uncertainties in the actual value of the diffusion coefficient of ^{22}Ne (Deloye & Bildsten 2002), we compute additional cooling sequences altering the diffusion coefficient by a factor of 2. Finally, we find it worthwhile to assess the lowest metallicity for which ^{22}Ne sedimentation starts to affect significantly the cooling times of white dwarfs. To this end, we compute additional cooling sequences for initial ^{22}Ne abundances of 0.01 and 0.005.

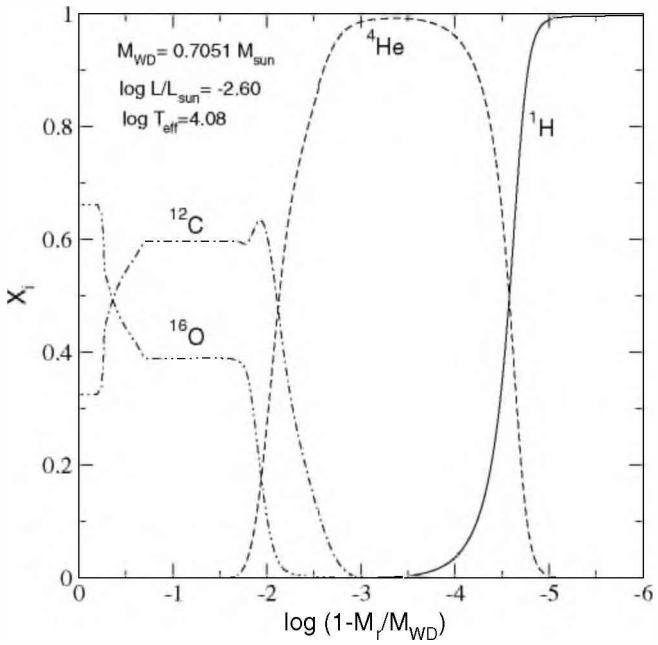

Figure 1. Chemical abundance distribution (carbon, oxygen, hydrogen, and helium) for a selected 0.7051 $M_{\odot}$ white dwarf model after element diffusion has led to the formation of a pure hydrogen envelope.

3. RESULTS

The results presented in this work are based on a complete and consistent treatment of the different energy sources that influence the evolution of white dwarfs along the distinct evolutionary stages. The ultimate aim is to provide cooling ages that are as accurate as possible, according to our best knowledge of the physical processes that drive the evolution of these stars. In particular, we compute here the first grid of white dwarf

Table 1
Initial and Final Stellar Mass (in Solar Units), and the Central Oxygen Abundance (Mass Fraction) of Our Starting White Dwarf Sequences

M_{WD}	M_{ZAMS}	X_O
0.5249	1.00	0.70
0.5701	1.50	0.68
0.5932	1.75	0.70
0.6096	2.00	0.72
0.6323	2.25	0.75
0.6598	2.50	0.72
0.7051	3.00	0.66
0.7670	3.50	0.65
0.8779	5.00	0.61

Note. The progenitor metallicity is $Z = 0.01$.

evolutionary sequences that incorporates the sedimentation of ^{22}Ne. The grid is intended for applications to white dwarfs with high ^{22}Ne abundances in their cores, namely, those resulting from metal-rich progenitors, for which ^{22}Ne sedimentation is expected to impact their evolution. In the interest of avoiding a lengthy discussion of the results, we will focus on the consequences of ^{22}Ne sedimentation on the evolution, postponing a comprehensive description of the standard evolutionary aspects, particularly the role of carbon–oxygen phase separation, to a companion publication (Renedo et al. 2010).

As shown by Deloye & Bildsten (2002) and García-Berro et al. (2008), ^{22}Ne sedimentation is a slow process that impacts the evolution of white dwarfs only after long enough times have elapsed. During the evolutionary stages where most of the white dwarf remains in a liquid state, this process causes a strong depletion of ^{22}Ne in the outer region of the core, and an enhancement of its abundance in the central regions of the star. This behavior becomes substantially more noticeable as the gravity is increased. Indeed, a more rapid sedimentation and a faster depletion of ^{22}Ne in the outer layers is expected in massive white dwarfs. However, because massive white dwarfs crystallize earlier than less massive ones, ^{22}Ne sedimentation will stop at higher effective temperatures as compared with less massive white dwarfs, thus limiting the extent to which ^{22}Ne diffusion constitutes an energy source for the star. This is a critical issue regarding the cooling behavior of massive white dwarfs.

As expected, the contribution of ^{22}Ne sedimentation to the luminosity budget of white dwarfs becomes larger as the metal content of the parent star is increased. This is exemplified in Figure 2, which shows the resulting luminosity contribution (expressed in solar units) in terms of the effective temperature of the white dwarf for the 0.7051 and the 0.5249 $M_\odot$ sequences (upper and bottom panels, respectively) and for the two metallicities adopted in this work, $Z = 0.03$ and 0.06. This figure gives us a deep insight of the importance of ^{22}Ne sedimentation into the global energetics during the entire white dwarf evolution. Note that the contribution from this process to the star luminosity is notably enhanced in the case of more massive white dwarfs. Moreover, after the onset of core crystallization ^{22}Ne sedimentation is still a relevant process. As the core becomes increasingly crystallized, the luminosity due to ^{22}Ne sedimentation declines steeply (at higher effective temperatures in more massive white dwarfs). For low-mass white dwarfs, the impact of ^{22}Ne sedimentation is markedly less noticeable, albeit not negligible in the case of high Z. In Figure 2, we also display (with thin solid lines) the luminosity

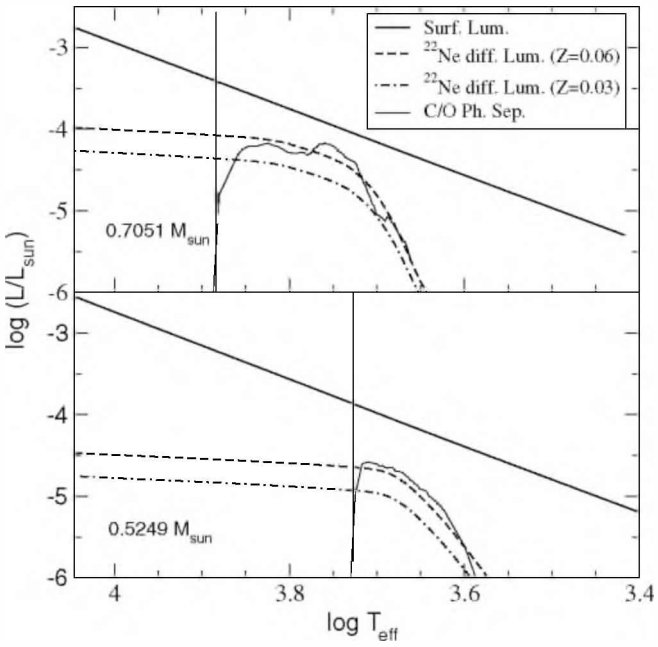

Figure 2. Luminosity contribution in solar units due to ^{22}Ne sedimentation vs. effective temperature for the 0.7051 and 0.5249 $M_\odot$ white dwarf sequences (upper and bottom panels, respectively), and for $Z = 0.06$ and 0.03 (dashed and dot-dashed lines), respectively. The solid line displays the surface luminosity and the thin solid line displays the luminosity contribution from carbon–oxygen phase separation. The vertical line marks the effective temperature for the onset of core crystallization.

contribution that results from carbon–oxygen phase separation. It can been seen that, depending on the stellar mass and metal content, the contribution of ^{22}Ne sedimentation to the energetics is comparable or larger than that resulting from carbon–oxygen phase separation.

It is clear that ^{22}Ne sedimentation plays a major role in the energetics of cool white dwarfs characterized by a high metal content in their interiors. The impact of this process as well as of latent heat and carbon–oxygen phase separation in the white dwarf cooling ages can be seen in Figures 3 and 4 for the case of $Z = 0.03$ and 0.06, respectively. Here, the white dwarf surface luminosity is shown as a function of the age. In each figure, the upper and bottom panels correspond to the 0.5249 and 0.7051 $M_\odot$ sequences, respectively. The solid line corresponds to the standard case in which latent heat is considered, and carbon–oxygen phase separation and ^{22}Ne sedimentation are neglected. The inclusion of ^{22}Ne sedimentation strongly modifies the cooling curves (dashed lines). Finally, the addition of the energy resulting from carbon–oxygen phase separation upon crystallization (and ^{22}Ne sedimentation) gives rise to the cooling curve shown as a dot-dashed line. Clearly, the energy released by ^{22}Ne sedimentation markedly influences the cooling times, particularly those of the more massive white dwarfs. Note that in this case, the magnitude of the delays in the cooling rates resulting from ^{22}Ne sedimentation is comparable (or even much larger in the case of $Z = 0.06$) to the delays induced by carbon–oxygen phase separation.

According to what we have discussed, the signatures of ^{22}Ne sedimentation in the cooling rate will certainly be different depending on the mass of the white dwarf. In particular, because of their larger gravities, they start to manifest themselves earlier in more massive white dwarfs. This can be better appreciated in Figure 5, where we show the cooling curves for the 0.5249,

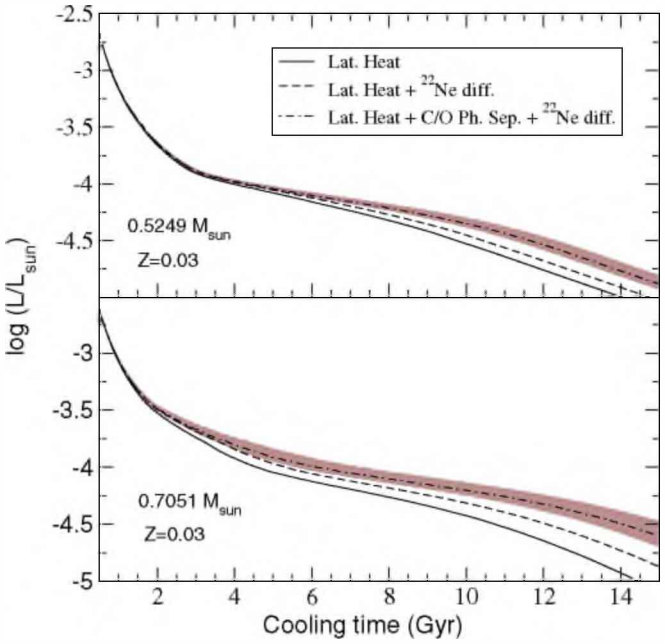

Figure 3. Surface luminosity vs. age for the 0.5249 and 0.7051 $M_{\odot}$ sequences (upper and bottom panels, respectively). The solid line displays the cooling times for the case in which only the release of latent heat is considered and carbon–oxygen phase separation and ^{22}Ne sedimentation are neglected. The dashed line displays the results for the case where both latent heat and ^{22}Ne sedimentation are included, but not carbon–oxygen phase separation. The dot-dashed line corresponds to the case where latent heat, carbon–oxygen phase separation, and ^{22}Ne sedimentation are considered. For this case, the gray region shows the extent to which the cooling times change when the diffusion coefficient of ^{22}Ne is changed by a factor of 2. The metal content in all cases is $Z = 0.03$.

(A color version of this figure is available in the online journal.)

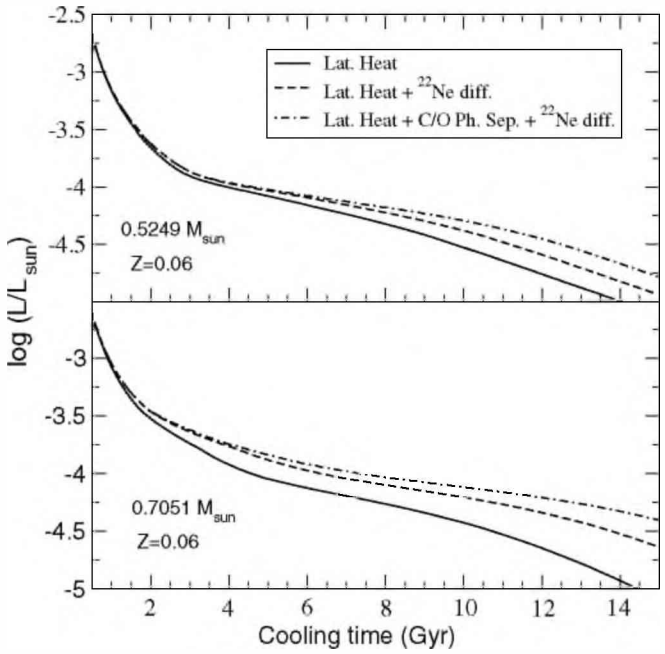

Figure 4. Similar to Figure 3 but for white dwarf models with a metal content of Z = 0.06 in their cores.

0.7051, and 0.8779 $M_{\odot}$ sequences for the case $Z = 0.03$. In both panels, we display with thick lines the cooling curves that result from considering the energy released by crystallization (latent heat), carbon–oxygen phase separation, and ^{22}Ne sedimentation.

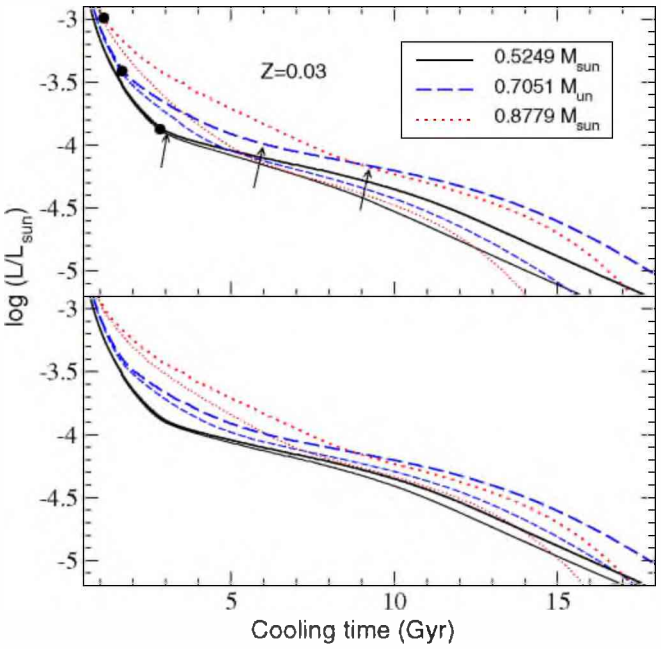

Figure 5. Surface luminosity vs. cooling time for the 0.5249, 0.7051, and 0.8779 $M_{\odot}$ sequences. In both panels, the thick lines correspond to sequences where the release of latent heat, carbon–oxygen phase separation, and ^{22}Ne sedimentation are considered. Sequences with thin lines consider either only latent heat (upper panel) or latent heat plus carbon–oxygen separation (bottom panel), but not ^{22}Ne sedimentation. Filled circles and arrows at selected sequences denote, respectively, the onset of crystallization and the time at which convective coupling occurs. The metallicity is $Z = 0.03$.

(A color version of this figure is available in the online journal.)

The thin lines show the corresponding cooling curves when ^{22}Ne sedimentation is neglected, but latent heat (upper panel) and latent heat and carbon–oxygen phase separation (bottom panel) are taken into account. Note the marked lengthening of the cooling times that results from the occurrence of ^{22}Ne sedimentation at luminosities as high as $\log(L/L_{\odot}) \approx -3.5$ (see the bottom panel) for the massive sequence of 0.8779 $M_{\odot}$. This delay persists until low luminosities. For the lowest stellar masses considered in this work (0.5249 $M_{\odot}$), appreciable delays in the cooling rates due to ^{22}Ne sedimentation take place, but only at luminosities lower than $\log(L/L_{\odot}) \approx -4.2$. Carbon–oxygen phase separation also leads to appreciable delays in the cooling rates. The extent of this delay and the luminosities at which this occurs depend on the stellar mass. In the case of more massive white dwarfs, most of the carbon–oxygen phase separation and ^{22}Ne sedimentation occur during evolutionary stages prior to the convective coupling—the onset of which is indicated by arrows on the sequences with thick lines in the upper panel. Convective coupling takes places when the envelope convective region penetrates into the degenerate core, with the consequent release of excess thermal energy, and the resulting slowdown of the cooling process, as reflected by the change of slope in the cooling curve (see Fontaine et al. 2001). By contrast, in the less massive models, the delay in the cooling rate due to convective coupling takes place before the release of appreciable energy from carbon–oxygen phase separation and ^{22}Ne sedimentation. This in part helps to understand the distinct behavior of the cooling curves with stellar mass.

From the preceding paragraphs, we conclude that, in the case of white dwarfs that result from progenitor stars with supersolar metallicity, the occurrence of ^{22}Ne sedimentation releases enough energy to produce appreciable delays in the rate

Table 2
Differences in the Evolutionary Times (Gyr) between Sequences which Include the Release of Latent Heat, Carbon–Oxygen Phase Separation, and ^{22}Ne Sedimentation with the Sequence which Considers Only the Release of Latent Heat

	$Z = 0.03$							$Z = 0.06$						
$\log(L/L_\odot)$	0.5249	0.5932	0.6598	0.7051	0.7670	0.8779	1.0000	0.5249	0.5932	0.6598	0.7051	0.7670	0.8779	1.0000
−3.0	<0.01	0.01	0.01	0.02	0.03	0.07	0.35	0.01	0.02	0.03	0.03	0.05	0.14	0.67
−3.5	0.03	0.05	0.10	0.14	0.33	1.02	1.45	0.07	0.09	0.20	0.30	0.64	1.80	2.61
−4.0	0.38	0.64	1.03	1.63	2.04	2.51	2.30	0.66	1.18	1.89	2.88	3.58	4.26	3.79
−4.5	1.90	2.44	2.84	3.31	3.33	3.20	2.60	2.73	3.69	4.43	5.29	5.33	5.05	4.10

Note. The results are shown at selected stellar luminosities and masses (in solar units), for both $Z = 0.03$ and $Z = 0.06$.

of cooling at relevant stellar luminosities. We can obtain a more quantitative idea of this assertion examining Figure 6—see also Table 2—which shows the age difference between sequences that incorporate the energy released from ^{22}Ne sedimentation and the sequence that considers only latent heat, for two masses and the two metallicities adopted in this study. It is clear that both carbon–oxygen phase separation and ^{22}Ne sedimentation lead to substantial delays in the cooling times. Note that, at very low surface luminosities and for metallicity $Z = 0.03$, the inclusion of both carbon–oxygen phase separation and ^{22}Ne sedimentation produces age differences between ∼2.0 and 3.3 Gyr, depending on the value of the stellar mass. These differences range from 2.7 to 5.3 Gyr for the case of progenitor stars with $Z = 0.06$. Note also that the magnitude of the delay resulting from the ^{22}Ne sedimentation is comparable or even larger than that induced by carbon–oxygen phase separation. In particular, by $\log(L/L_\odot) \approx -4.0$, the luminosity at which the faint peak of the white dwarf luminosity function in NGC 6791 is located, the release of energy from ^{22}Ne sedimentation markedly slows down the cooling rate of the more massive white dwarfs, which, because of their short pre-white-dwarf times, populate the faint end of the white dwarf luminosity function of the cluster. For our more massive sequences and at the metallicity of the cluster ($Z \simeq 0.04$), we find that the delays from ^{22}Ne sedimentation alone range from 1.10 to 1.50 Gyr and ≈ 1.80 Gyr at $\log(L/L_\odot) \approx -4.0$ and −4.2, respectively. These delays together with the delays resulting from carbon–oxygen phase separation, are on the order of what is required to solve the age discrepancy in NGC 6791 (García-Berro et al. 2010). The delay in the cooling rate of white dwarfs resulting from ^{22}Ne sedimentation is important and points out the necessity of incorporating this energy source in the calculation of detailed white dwarf cooling sequences, particularly in the case of white dwarfs populating metal-rich clusters.

Because of the relevance of the ^{22}Ne sedimentation for the cooling of white dwarfs, we find it instructive to estimate the lowest metallicity for which ^{22}Ne sedimentation starts to affect significantly the cooling times of white dwarfs. To this end, we compute additional cooling sequences for initial ^{22}Ne abundances of 0.01 and 0.005. For the case of an initial ^{22}Ne abundance of 0.01, ^{22}Ne sedimentation increases the cooling time of our 0.5249 $M_\odot$ sequence that considers latent heat and carbon–oxygen phase separation by at most 1%–2%. The magnitude of the delays is larger for more massive white dwarfs, reaching 3%–6% and 4%–8% for the 0.7051 and 1.0 $M_\odot$ sequences, respectively. For these two stellar masses, the resulting delays are 1.5%–3% and 2%–4% for ^{22}Ne abundances of 0.005. We conclude that, for initial ^{22}Ne abundances smaller than ≈0.01, ^{22}Ne sedimentation has a minor impact on white dwarf cooling times, except for rather massive white dwarfs for

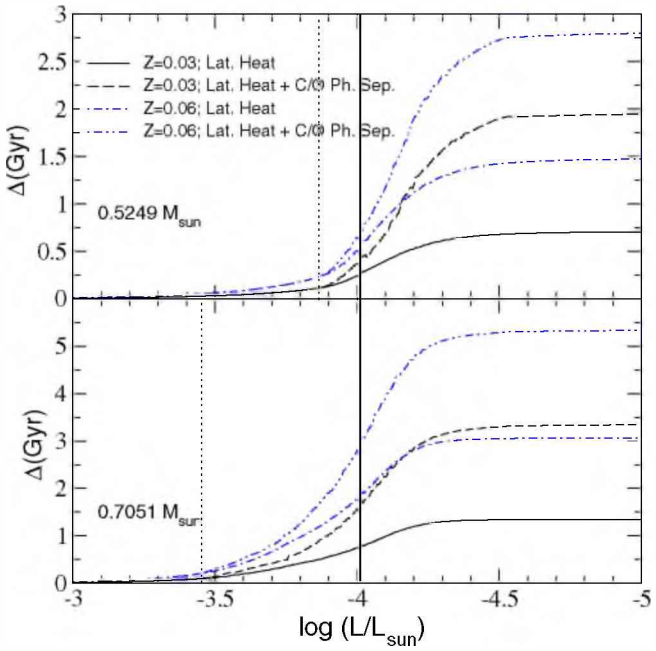

Figure 6. Difference in evolutionary times (Gyr) between various sequences that include ^{22}Ne diffusion and the sequence which considers only latent heat, for white dwarfs with masses 0.5249 and 0.7051 $M_\odot$. The vertical dotted lines mark the surface luminosity at the onset of core crystallization and the vertical solid line marks the location of the faint peak in the NGC 6791 luminosity function.

(A color version of this figure is available in the online journal.)

which non-negligible delays (but smaller than 8%) are found even for ^{22}Ne abundances of 0.005.

Finally, to account for possible uncertainties in the actual value of the diffusion coefficient of ^{22}Ne (Deloye & Bildsten 2002), we compute additional cooling sequences for which we multiply and divide the diffusion coefficient by a factor of 2. The resulting impacts on the cooling time for the case in which $Z = 0.03$ can be seen in Figure 3 for the 0.7051 and 0.5249 $M_\odot$ sequences that consider latent heat, carbon–oxygen phase separation, and ^{22}Ne sedimentation. The gray region shows the extent to which the cooling curves vary when the diffusion coefficient is changed within this range of values. For the more massive sequence and at $\log(L/L_\odot) = -4.5$ and −4, the cooling times change by less than 8% and −5%, and by 17% and −8%, respectively. For the less massive sequence, the changes remain below 7%. In the case of the 1.0 $M_\odot$ sequence, an increase in D_s by a factor of 2 causes a maximum age difference of ≈20% in the luminosity range from $\log(L/L_\odot) \approx -3$ to −3.5. It is clear that uncertainties in the diffusion coefficient larger than a factor of 2 will affect

the cooling time considerably, particularly for our most massive white dwarf sequences.

4. CONCLUSIONS

The use of white dwarfs as reliable cosmic clocks to date Galactic stellar populations has been recently thrown into doubt by a new observational determination of the white dwarf luminosity function in the old, metal-rich open cluster NGC 6791 (Bedin et al. 2008), the age of which as derived from the main-sequence turnoff technique (8 Gyr) markedly disagrees with the age derived from the termination of the white dwarf cooling sequence (6 Gyr). This discrepancy points out at a missing physical process in the standard treatment of white dwarf evolution. In view of the high metallicity characterizing NGC 6791 ($Z \approx 0.04$), the gravitational settling of ^{22}Ne constitutes the most viable process that can decrease the cooling rate of cool white dwarfs. Indeed, as first shown by Isern et al. (1991) and later by Deloye & Bildsten (2002) and García-Berro et al. (2008), the slow gravitational settling of ^{22}Ne in the liquid phase releases enough energy as to appreciably slow down the cooling rate of white dwarfs in metal-rich clusters like NGC 6791.

Motivated by these considerations, we have presented a grid of white dwarf evolutionary sequences that incorporates for the first time the energy contributions arising from both ^{22}Ne sedimentation and carbon–oxygen phase separation. The grid covers the entire mass range expected for carbon–oxygen white dwarfs, from 0.52 to 1.0 $M_{\odot}$, and is based on a detailed and self-consistent treatment of these energy sources. Except for the 1.0 $M_{\odot}$ sequence, the history of progenitor stars has been taken into account by evolving initial stellar configurations in the mass range 1–5 $M_{\odot}$ from the ZAMS all the way through the TP-AGB and mass-loss phases. Because of the full calculation of the evolution of progenitor stars, the white dwarf sequences incorporate realistic and consistent carbon–oxygen profiles—of relevance for an accurate computation of the energy released by carbon–oxygen phase separation. In addition, detailed non-gray model atmospheres are used to derive the outer boundary condition for the evolving sequences. At the low luminosities where the process of ^{22}Ne sedimentation becomes relevant, the outer boundary conditions influence the cooling times.

We find that ^{22}Ne sedimentation has notable consequences for the cooling times of cool white dwarfs characterized by a high metal content in their interiors. The related energy release strongly delays their cooling. The precise value of the delays depends on the mass of the white dwarf, its luminosity, and on the metal content. For instance, because of their larger gravities, the impact of ^{22}Ne sedimentation starts earlier in more massive white dwarfs. In particular, appreciable delays in the cooling rates start to manifest themselves at luminosities of $\log(L/L_{\odot}) \approx -3.5$ to -4.2. In general, the magnitude of the delays in the cooling rates resulting from ^{22}Ne sedimentation is comparable (or even larger in the case of $Z = 0.06$) to the delays induced by carbon–oxygen phase separation. At the approximate location of the faint peak in the white dwarf luminosity function of NGC 6791, delays between 1 and 1.5 Gyr are expected as a result of ^{22}Ne sedimentation only. As recently shown in García-Berro et al. (2010), the occurrence of this process in the interior of cool white dwarfs is a key factor in solving the longstanding age discrepancy of NGC 6791.

In summary, we find that the evolution of cool white dwarfs stemming from progenitor stars with supersolar metallicity is strongly modified by the energy released from ^{22}Ne sedimentation. The resulting delays in cooling times of such white dwarfs are important and have to be taken into account in age determinations of metal-rich clusters from the cooling sequence of their white dwarfs. The grid of evolutionary sequences we have presented here is the first one intended for such a purpose, and incorporates the effects carbon–oxygen phase separation and ^{22}Ne sedimentation in the evolution of these stars.

We acknowledge the comments and suggestions of our referee, which help us to improve the original version of this paper. This research was supported by AGAUR, MCINN grant AYA2008-04211-C02-01, the European Union FEDER funds, AGENCIA: Programa de Modernización Tecnológica BID 1728/OC-AR, and PIP 2008-00940 from CONICET. L.G.A. also acknowledges a PIV grant of the AGAUR of the Generalitat de Catalunya.

REFERENCES

Alexander, D. R., & Ferguson, J. W. 1994, ApJ, 437, 879
Althaus, L. G., García-Berro, E., Isern, J., & Córsico, A. H. 2005a, A&A, 441, 689
Althaus, L. G., García-Berro, E., Isern, J., Córsico, A. H., & Rohrmann, R. D. 2007, A&A, 465, 249
Althaus, L. G., Miller Bertolami, M. M., Córsico, A. H., García-Berro, E., & Gil-Pons, P. 2005b, A&A, 440, L1
Althaus, L. G., Panei, J. A., Miller Bertolami, M. M., García-Berro, E., Córsico, A. H., Romero, A. D., Kepler, S. O., & Rohrmann, R. D. 2009a, ApJ, 704, 1605
Althaus, L. G., Panei, J. A., Romero, A. D., Rohrmann, R. D., Córsico, A. H., García-Berro, E., & Miller Bertolami, M. M. 2009b, A&A, 502, 207
Althaus, L. G., Serenelli, A. M., Córsico, A. H., & Montgomery, M. H. 2003, A&A, 404, 593
Angulo, C., et al. 1999, Nucl. Phys. A, 656, 3
Bedin, L. R., King, I. R., Anderson, J., Piotto, G., Salaris, M., Cassisi, S., & Serenelli, A. 2008, ApJ, 678, 1279
Bravo, E., Isern, J., Canal, R., & Labay, J. 1992, A&A, 257, 534
Cassisi, S., Potekhin, A. Y., Pietrinferni, A., Catelan, M., & Salaris, M. 2007, ApJ, 661, 1094
Catalán, S., Isern, J., García-Berro, E., & Ribas, I. 2008, MNRAS, 387, 1693
Caughlan, G. R., & Fowler, W. A. 1988, At. Data Nucl. Data Tables, 40, 283
Deloye, C. J., & Bildsten, L. 2002, ApJ, 580, 1077
Fontaine, G., Brassard, P., & Bergeron, P. 2001, PASP, 113, 409
García-Berro, E., Althaus, L. G., Córsico, A. H., & Isern, J. 2008, ApJ, 677, 473
García-Berro, E., Hernanz, M., Isern, J., & Mochkovitch, R. 1988a, Nature, 333, 642
García-Berro, E., Hernanz, M., Isern, J., & Mochkovitch, R. 1988b, A&A, 193, 141
García-Berro, E., Torres, S., Isern, J., & Burkert, A. 1999, MNRAS, 302, 173
García-Berro, E., et al. 2010, Nature, 465, 194
Grevesse, N., & Sauval, A. J. 1998, Space Sci. Rev., 85, 161
Guandalini, R., Busso, M., Ciprini, S., Silvestro, G., & Persi, P. 2006, A&A, 445, 1069
Haft, M., Raffelt, G., & Weiss, A. 1994, ApJ, 425, 222
Hansen, B. M. S., et al. 2002, ApJ, 574, L155
Hansen, B. M. S., et al. 2007, ApJ, 671, 380
Hernanz, M., García-Berro, E., Isern, J., Mochkovitch, R., Segretain, L., & Chabrier, G. 1994, ApJ, 434, 652
Herwig, F., Blöcker, T., Schönberner, D., & El Eid, M. 1997, A&A, 324, L81
Iglesias, C. A., & Rogers, F. J. 1996, ApJ, 464, 943
Isern, J., García-Berro, E., Hernanz, M., & Chabrier, G. 2000, ApJ, 528, 397
Isern, J., García-Berro, E., Hernanz, M., Mochkovitch, R., & Torres, S. 1998, ApJ, 503, 239
Isern, J., Mochkovitch, R., García-Berro, E., & Hernanz, M. 1991, A&A, 241, L29
Isern, J., Mochkovitch, R., García-Berro, E., & Hernanz, M. 1997, ApJ, 485, 308
Itoh, N., Hayashi, H., Nishikawa, A., & Kohyama, Y. 1996, ApJS, 102, 411
Kippenhahn, R., & Weigert, A. 1990, Stellar Structure and Evolution (Heidelberg: Springer)
Lamb, D. Q., & Van Horn, H. M. 1975, ApJ, 200, 306
Marigo, P., & Aringer, B. 2009, A&A, 508, 1539

Mestel, L. 1952, MNRAS, 112, 583
Miller Bertolami, M. M., & Althaus, L. G. 2006, A&A, 454, 845
Miller Bertolami, M. M., Althaus, L. G., Unglaub, K., & Weiss, A. 2008, A&A, 491, 253
Montgomery, M. H., Klumpe, E. W., Winget, D. E., & Wood, M. A. 1999, ApJ, 525, 482
Prada Moroni, P. G., & Straniero, O. 2002, ApJ, 581, 585
Prada Moroni, P. G., & Straniero, O. 2007, A&A, 466, 1043
Renedo, I., Althaus, L. G., Miller Bertolami, M. M., Romero, A. D., Córsico, A. H., Rohrmann, R., & García-Berro, E. 2010, ApJ, 717, 183
Richer, H. B., et al. 1997, ApJ, 484, 741
Rohrmann, R. D., Althaus, L. G., & Kepler, S. O. 2010, MNRAS, submitted
Rohrmann, R. D., Serenelli, A. M., Althaus, L. G., & Benvenuto, O. G. 2002, MNRAS, 335, 499
Salaris, M., Cassisi, S., Pietrinferni, A., Kowalski, P. M., & Isern, J. 2010, ApJ, 716, 1241
Salaris, M., Domínguez, I., García-Berro, E., Hernanz, M., Isern, J., & Mochkovitch, R. 1997, ApJ, 486, 413
Salaris, M., Serenelli, A., Weiss, A., & Miller Bertolami, M. M. 2009, ApJ, 692, 1013
Schröder, K.-P., & Cuntz, M. 2005, ApJ, 630, L73
Segretain, L. 1996, A&A, 310, 485
Segretain, L., & Chabrier, G. 1993, A&A, 271, L13
Segretain, L., Chabrier, G., Hernanz, M., García-Berro, E., & Isern, J. 1994, ApJ, 434, 641
Stevenson, D. J. 1980, J. Phys. Suppl., 41, C61
Straniero, O., Domínguez, I., Imbriani, G., & Piersanti, L. 2003, ApJ, 583, 878
Torres, S., García-Berro, E., Burkert, A., & Isern, J. 2002, MNRAS, 336, 971
Unglaub, K., & Bues, I. 2000, A&A, 359, 1042
Van Horn, H. M. 1968, ApJ, 151, 227
Vassiliadis, E., & Wood, P. R. 1993, ApJ, 413, 641
Von Hippel, T., & Gilmore, G. 2000, AJ, 120, 1384
Von Hippel, T., Jefferys, W. H., Scott, J., Stein, N., Winget, D. E., DeGennaro, S., Dam, A., & Jeffery, E. J. 2006, ApJ, 645, 1436
Weiss, A., & Ferguson, J. W. 2009, A&A, 508, 1343
Winget, D. E., Hansen, C. J., Liebert, J., Van Horn, H. M., Fontaine, G., Nather, R. E., Kepler, S. O., & Lamb, D. Q. 1987, ApJ, 315, L77
Winget, D. E., Kepler, S. O., Campos, F., Montgomery, M. H., Girardi, L., Bergeron, P., & Williams, K. 2009, ApJ, 693, L6